Journal of Applied Electrochemistry **32**: 1005–1010, 2002.

Kinetics of hydrogen evolution on submicron size Co, Ni, Pd and Co–Ni alloy powder electrodes by d.c. polarization and a.c. impedance studies

P. ELUMALAI[1], H.N. VASAN[1,*], N. MUNICHANDRAIAH[2,*] and S.A. SHIVASHANKAR[3]
[1]*Solid State and Structural Chemistry Unit, Indian Institute of Science, Bangalore, 560 012, India*
[2]*Inorganic and Physical Chemistry, Indian Institute of Science, Bangalore, 560 012, India*
[3]*Materials Research Center, Indian Institute of Science, Bangalore, 560 012, India*
*(*authors for correspondence, e-mails: vasan@sscu.iisc.ernet.in or muni@ipc.iisc.ernet.in)*

Received 17 December 2001; accepted in revised form 11 June 2002

Key words: a.c. impedance, d.c. polarization, hydrogen evolution, submicron size particles

Abstract

Submicron size Co, Ni and Co–Ni alloy powders have been synthesized by the polyol method using the corresponding metal malonates and Pd powder by reduction of PdO_x in methanol. The kinetics of the hydrogen evolution reaction (HER) in 6 M KOH electrolyte have been studied on electrodes made from the pressed powders. The d.c. polarization measurements have resulted in a value close to 120 mV decade^{-1} for the Tafel slope, suggesting that the HER follows the Volmer–Heyrovsky mechanism. The values of exchange current density (i_o) are in the range 1–10 mA cm^{-2} for electrodes fabricated in the study. The a.c. impedance spectra measured at several potentials in the HER region showed a single semicircle in the Nyquist plots. Exchange current density (i_o) and energy transfer coefficient (α) have been calculated by employing a nonlinear least square-fitting program.

1. Introduction

The hydrogen evolution reaction (HER) on electrode surfaces is a fundamental process that has been studied over many years [1–3]. Various transition metals, especially Raney nickel, prepared by leaching of Al or Zn, are known to be very effective catalysts for this purpose [4], as also are various alloy systems, for example, Ni–Mo, Ni–Zn, Ni–W, Ni–Fe, Ni–Cr and Ni–Al electrodes made by powder pressing, electrodeposition or leaching [5–8]. From kinetic studies it has been found that Ni–Mo alloy powder is a promising cathode for the HER in alkaline medium [8]. To the authors' knowledge, there are only few HER studies using electrodes made of small metal/alloy particles; for example, Ni or Ni–B alloys [9–11] and also very few studies on electrodes based on cobalt [12–14] and palladium [15–17]. Small metal/alloy particles in the nano- to micrometre range may be obtained by low temperature routes using polyol [18] or simple alcohols. We have synthesized nanoparticles of Ag–Pd and Cu–Pd alloys using ethyl alcohol [19] and have reported the electrochemical activity of these alloys for methanol oxidation [20]. Here we report the kinetics of HER on electrodes made from submicron size powders of Co, Pd, Ni and Co–Ni alloys synthesized by the polyol method as well as on physical mixtures of Co–Pd.

2. Experimental details

Pure metal powders of Co and Ni, as well as Co–Ni alloys of different compositions were synthesized by the polyol method using the corresponding metal malonates. A detailed procedure has been described elsewhere [21]. In brief, the metal malonates were prepared by dissolving the corresponding metal hydroxides, (which in turn was prepared by adding potassium hydroxide to the metal nitrate solution) in malonic acid (all the chemicals used were AR grade, s.d. fine chemicals). The respective metal malonates (1.0 g) were then refluxed in ethylene glycol (200 ml) for 2–6 h in nitrogen atmosphere. During this process, reduction of the metal ion occurs, producing submicron size metal powder. The powder was washed in deaerated water and methanol, and preserved in methanol for further studies. For the synthesis of Co–Ni alloys, the corresponding metal malonate mixtures in the required ratio were refluxed in ethylene glycol. Pd powder was synthesized by reduction of PdO_x obtained by decomposition of $Pd(NO_3)_2$ (Aldrich), on refluxing with methanol (Qualigen AR grade). As Co–Pd alloy powders could not be obtained by this procedure, physical mixtures of the corresponding metal powders in the required composition were obtained by mechanical mixing.

For electrochemical studies, a thin (0.1 mm), circular (dia. 3 mm) pellet-type electrode with a geometrical area

of 0.2 cm^2 (both sides combined) were made by compacting 20 mg of metal powder or alloy, or a mixture of metals at a pressure of 5 kN for 5 min. Nickel wire was embedded into the powder before pressing for the purpose of electrical contact. The electrode was then inserted symmetrically between two large (3.8 cm × 3.5 cm) nickel-sheet auxiliary electrodes into a glass electrochemical cell containing a solution of 6 M KOH, prepared by dissolving analytical grade KOH in double distilled water. The electrolyte was preelectrolysed using Pt electrodes overnight. Electrode potentials were recorded and are reported against a Hg/HgO, OH^- reference electrode. Prior to the measurements, the electrode was cathodically polarized at a current density of 0.5 A cm^{-2} for about 5 h and allowed to attain equilibrium for several hours after cessation of current flow. This was done to reduce the surface oxide, if any, on the electrode. Steady-state galvanostatic polarization in the H_2 atmosphere was carried out using a regulated d.c. power source, a high resistance, and an ammeter in series with the electrochemical cell. Electrode potential was measured by means of a digital multimeter (Philips model PP 9007 true RMS multimeter) of high input impedance. Polarization curves were corrected for the uncompensated solution resistance measured by a.c. impedance. A.c. impedance data were measured in the frequency range 100 kHz to 10 mHz at an excitation signal of 5 mV using a computer controlled electrochemical impedance analyser (EG&G PARC model 6310). The impedance data were analysed by the Boukamp NLLS fitting program supplied by EG&G PARC [22].

3. Results and discussion

3.1. *Physical characterization of metal powders*

The XRD patterns of Co, Ni and $Co_{0.5}Ni_{0.5}$ powders (Figure 1) show clearly the formation of pure phases of the metals and alloys. The crystallite size, calculated using the Scherer formula (Equation 1) from the FWHM of (1 1 1) reflection, varies from 0.2 to 0.3 μm.

$$L_{hkl} = \frac{0.9\,\lambda}{\beta \cos\theta} \tag{1}$$

where L_{hkl} is average crystallite size (Å), λ is wave length of X-ray in angstroms, β is full width at half maximum (FWHM) in radians and θ is diffraction angle at (1 1 1). Representative SEM micrographs of Co power particles and of the pressed electrode made from Co, Co–Pd mixture of two composition are shown in Figure 2. It is seen that the Co particles are nonagglomerated and are almost spherical in shape. Crystal structure and crystallite size of the metal powders are given in Table 1.

3.2. *Hydrogen evolution reaction*

The mechanism of the HER in alkaline electrolyte is generally considered to consist of the following three steps [23–26]:

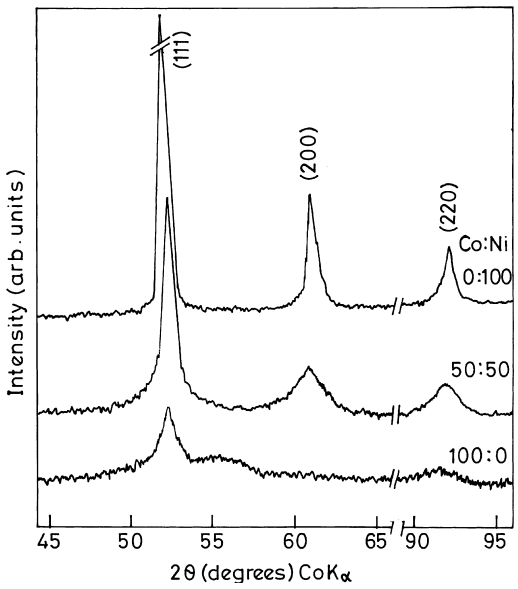

Fig. 1. Powder X-ray diffraction patterns of Co, Ni and $Co_{0.5}Ni_{0.5}$ alloy.

$$H_2O + M + e^- = MH_{ads} + OH^- \tag{2}$$

$$MH_{ads} + H_2O + e^- = M + OH^- + H_2 \uparrow \tag{3}$$

$$2\,MH_{ads} = 2M + H_2 \uparrow \tag{4}$$

The first step (Reaction 2), known as the Volmer reaction, is the primary electron transfer step resulting in the formation of adsorbed hydrogen (MH_{ads}) on the electrode surface from H_2O molecule. It is followed by the second step (Reaction 3), or/and the third step (Reaction 4), and the overall reaction is given by

$$2\,H_2O + 2\,e^- = H_2 + 2\,OH^- \tag{5}$$

Reaction 3, known as the Heyrovsky reaction, suggests the formation of H_2 molecule by desorption of surface hydrogen and a simultaneous reduction of H_2O molecule. Reaction 4, is called as the Tafel reaction, suggests the formation of an H_2 molecule by the combination of two neighboring adsorbed hydrogen atoms. A study of the literature suggests that HER on transition metals and alloys in alkaline electrolyte follows the Volmer–Heyrovsky mechanism, with the Volmer reaction as the rate-determining step (RDS) [23–26]. Therefore, here also we presume that the same mechanism is valid for the HER on Co, Pd, Ni and Co–Ni, Co–Pd electrodes. Under Tafel conditions (i.e., $(E - E^r) \gg RT/F$), the kinetic equation may be written as

$$\log i = \log i_o - \frac{\alpha f \eta}{2.303} \tag{6}$$

Thus, a graph of η against $\log i$ is expected to have a slope (the Tafel slope) of 120 mV ($= 2.303\ RT/\alpha F$) at 25 °C, assuming the value of $\alpha = 0.5$.

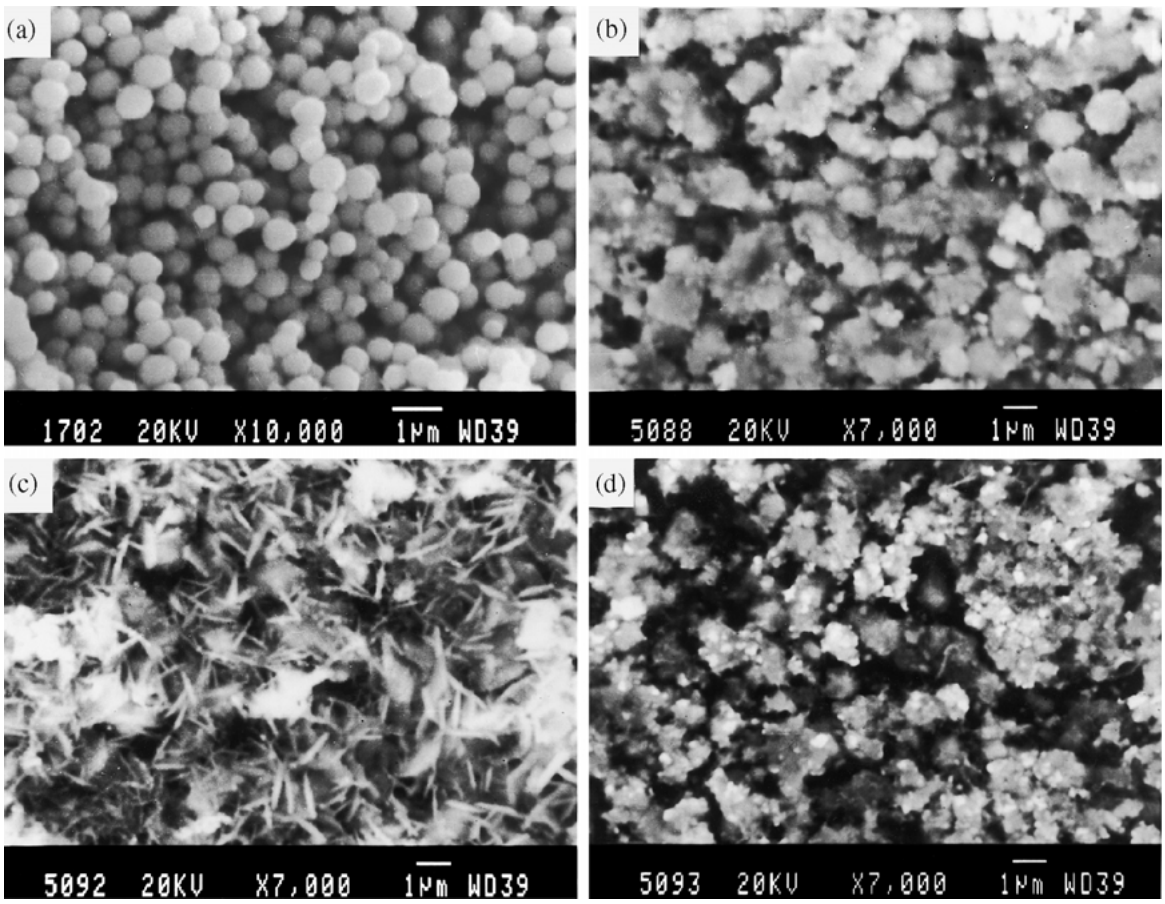

Fig. 2. SEMs of (a) cobalt metal powder, (b) Co, (c) 60Co:40Pd (mix) and (d) 40Co:60Pd (mix) pressed electrodes.

Table 1. Properties of metal/alloy particles

Metals/Alloys	Crystal structure	Crystallite size/μm
Co	FCC + HCP	0.20
Pd	FCC	0.21
Ni	FCC	0.30
$Co_{0.8}Ni_{0.2}$	FCC + HCP	0.20
$Co_{0.5}Ni_{0.5}$	FCC	0.20
$Co_{0.2}Ni_{0.8}$	FCC	0.22

Steady-state galvanostatic polarization of the electrodes in 6 M KOH was carried out. Typical Tafel plots for the Co, $Co_{0.5}Ni_{0.5}$ alloy and 40Co:60Pd mixture electrodes are shown in Figure 3. The plots are linear over about three orders of magnitude of current, with a Tafel slope close to 120 mV, which is theoretically expected for the Volmer–Heyrovsky mechanism. By extrapolation of the Tafel line to E^r ($= -0.93$ V), the

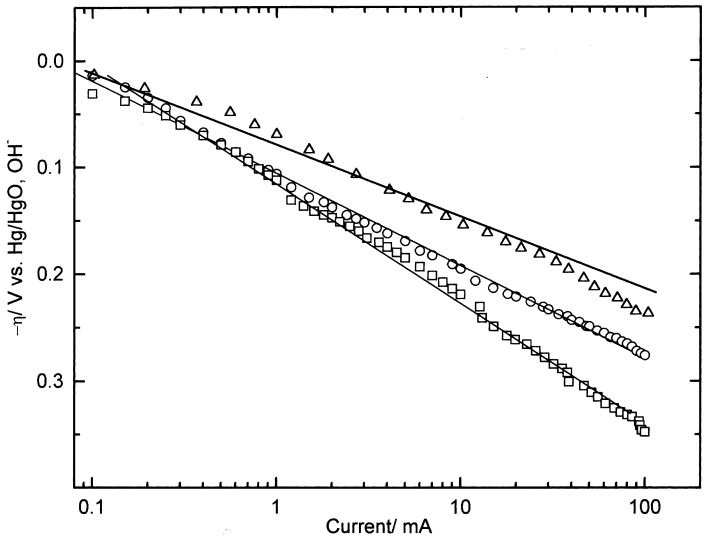

Fig. 3. Tafel plots for the representative electrodes in 6 M KOH. Key: (△) 40Co:60Pd (mix); (○) Co; (□) $Co_{0.5}Ni_{0.5}$.

exchange current densities (i_o) are obtained from Figure 3. It may be noted that the electrodes are porous (SEM picture) as they are made of submicron size particles. Hence the true surface area was expected to be higher than the geometrical area. The values of i_o, which was calculated on the basis of geometrical area, was termed the apparent exchange current density. The values of apparent i_o, the Tafel slope, the α and overpotential at 100 mA (η_{100}) of HER in 6 M KOH for electrodes in the study are tabulated in Table 2. The values of i_o are in the range 1–10 mA cm^{-2} for all electrodes. The mechanism of HER involves the formation of a M–H bond (step 2) as the RDS. It may be expected that the rate of this reaction, and hence the rate of HER, is greater if the free energy of adsorption of hydrogen is higher. However, this effect may render step 3 slower. Hence a cathode material should be such that it balances between Reactions 2 and 3 to achieve a higher rate of HER. A 'volcano plot' of i_o of the HER against the free energy of adsorption for a series of metal cathodes has been reported [27].

A.c. impedance spectra of the electrodes were recorded at several potentials between −0.93 V and −1.40 V; typical Nyquist plots for the Co electrode are shown in Figure 4. A single semicircle is observed in all the d.c. potentials. A study of the existing literature on a.c. impedance of HER on metal/alloy electrodes also show a single semicircle [4, 8, 17 and 28]. However, the semicircle obtained in the present study is distorted due to the porous nature of the electrode, as also observed by Chen and Lasia in Ni–Mo powder electrodes [8] and as proposed for rough electrodes by De Levie [29]. In a

Table 2. The values of Tafel slope, energy transfer coefficient (α), apparent exchange current density (i_o) and over potential at 100 mA (η_{100}) of the HER on various electrodes in 6 M KOH obtained from dc polarization measurements

Electrodes	Tafel slope /mV	α	i_o /mA cm^{-2}	η_{100} /mV
Co	98	0.61	1.1	274
Pd	96	0.62	1.4	297
Ni	101	0.59	1.2	328
$Co_{0.8}Ni_{0.2}$	107	0.56	1.2	341
$Co_{0.5}Ni_{0.5}$	128	0.46	1.3	266
$Co_{0.2}Ni_{0.8}$	130	0.46	1.4	334
80Co:20Pd (mix)	136	0.44	6.6	291
60Co:40Pd (mix)	147	0.40	6.3	285
40Co:60Pd (mix)	92	0.65	9.3	214

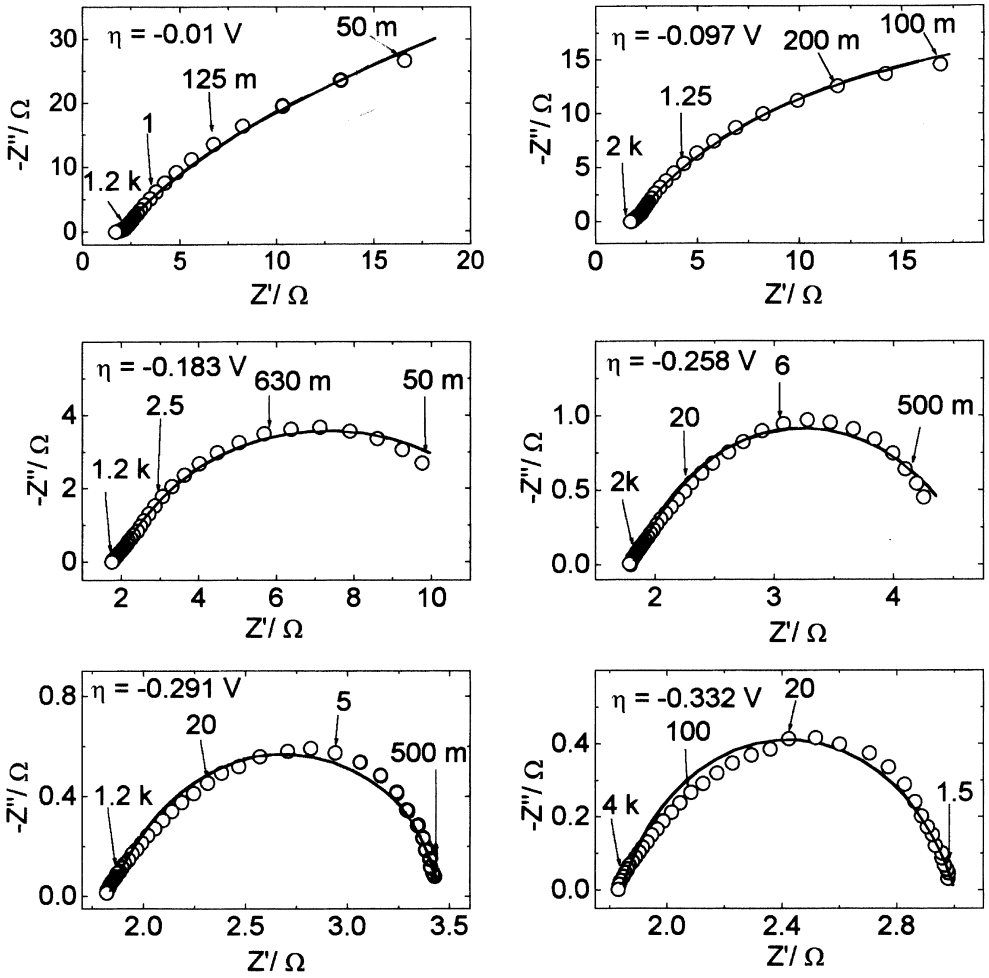

Fig. 4. Electrochemical a.c. impedance spectra in Nyquist form of Co electrode in 6 M KOH at different overpotentials (η against MMO). Experimental data shown as symbols and theoretical data obtained from NLLS fit results are shown as solid curves.

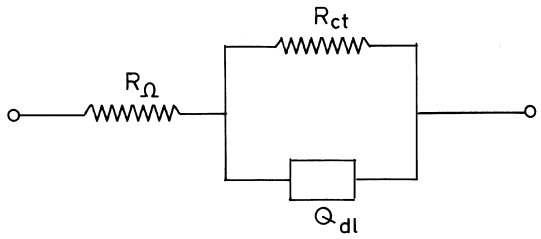

Fig. 5. Equivalent circuit used for NLLS fit. R_Ω, R_{ct} and Q_{dl} refer to ohmic resistance, charge-transfer resistance of HER and double-layer capacitance, respectively.

simple equivalent circuit model, the semicircle is considered due to the charge-transfer resistance (R_{ct}) of Reaction 2 and double-layer capacitance (C_{dl}) in parallel. The high frequency intercept provides the ohmic resistance of the cell, which is mainly due to the electrolyte resistance. For the purpose of evaluation of the impedance parameters, a nonlinear least squares (NLLS) fit procedure was employed [22] using the equivalent circuit shown in Figure 5 which includes uncompensated solution resistance (R_Ω) in series with the charge-transfer resistance (R_{ct}) of HER, which is in parallel with the constant phase elements (CPE) in place of capacitances. The admittance representation of the CPE is given by

$$Q(w) = Q_o(j\omega)^n \tag{7}$$

For $n = 0$, it represents a resistance with $R = Q_o^{-1}$; for $n = 1$, a capacitance with $C = Q_o$; for $n = 0.5$, a Warburg; and for $n = -1$ and inductance with $L = Q_o^{-1}$ [22].

The initial values required for the fitting were obtained using the Data Cruncher subprogram [22]. The impedance parameters obtained were assessed to be satisfactory by judging the correlation coefficients (not shown) and comparing the experimental impedance spectrum with that simulated using the fit results. Furthermore, the theoretical curves reasonably agree with experiment (Figure 4). The a.c. impedance spectra of all electrodes were also analysed by the NLLS fitting and the impedance parameters of the Co electrode at several potential values, for instance, are given Table 3.

Charge-transfer resistance (R_{ct}), is related to i_o and α of the HER as shown below [30]:

$$\ln R_{ct} + \ln(\alpha f i_o) = \alpha f \eta \tag{8}$$

Table 3. A.c. impedance parameters obtained by NLLS fitting for Co electrode made of fine particles in 6 M KOH at several potential values in the HER region

$-\eta$/V	0.01	0.097	0.183	0.258	0.291	0.332
R_Ω/Ω	1.81	1.83	1.83	1.83	1.85	1.84
$R_{ct}/\ \Omega\ cm^2$	29.64	7.96	2.14	0.51	0.32	0.16
$Q_{dl} \times 10^2/\Omega^{-1}$	8.31	4.53	4.42	3.29	2.44	1.76
n_{dl}	0.75	0.78	0.72	0.72	0.78	0.82

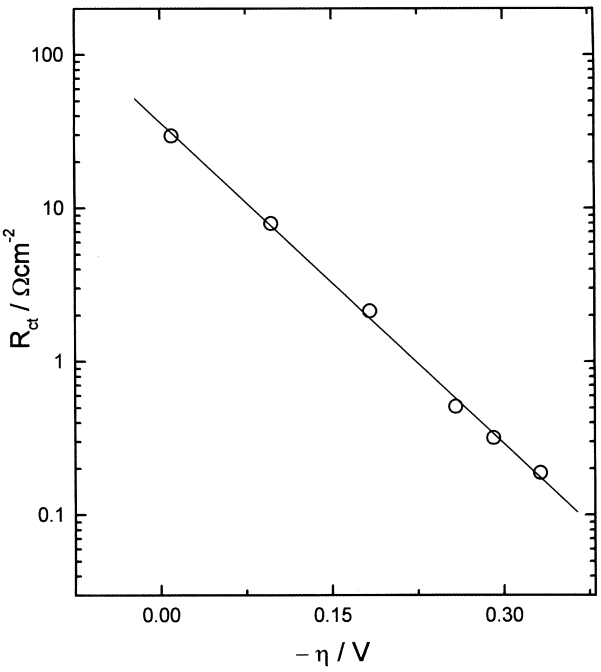

Fig. 6. Variation of charge-transfer resistance (R_{ct}) of HER as a function of overpotential (η) of cobalt electrode.

A plot of ln R_{ct} against η thus results in a straight line with a slope of (αf) and an intercept of $\ln(\alpha f i_o)^{-1}$. It is thus possible to evaluate α and i_o from the impedance spectra of the electrodes recorded in the HER potential regime. The variation of R_{ct} of the HER as a function of overpotential for a Co electrode is shown in Figure 6. There is a good linearity of the plot as expected from Equation 8. The values of apparent i_o and α derived are 1.9 mA cm^{-2} and 0.42, respectively. The values of i_o and α evaluated for all electrodes of the present study along with the n_{dl} value at $\eta = -0.33$ V are given in Table 4. The lower the values of n_{dl} the higher the porosity [8]. It is seen that the values of n_{dl} for Co–Pd (mix) are low compared to the individual metals and alloys indicating high porosity. This is further substantiated by the SEM micrographs (Figure 2(c) and (d)) of the mixture. Further, the higher activity towards the HER are seen in the overpotentials (η_{100}) and apparent exchange current densities. The kinetic parameters obtained from the a.c. impedance measurements are in reasonable

Table 4. Values of energy-transfer coefficient (α), exchange current density (i_o) and n_{dl} of the HER on various electrodes in 6 M KOH obtained from a.c. impedance measurements

Electrodes	α	i_o/mA cm^{-2}	n_{dl}
Co	0.42	1.9	0.82
Pd	0.34	6.1	0.7
Ni	0.30	4.0	0.71
$Co_{0.8}Ni_{0.2}$	0.26	3.1	0.66
$Co_{0.5}Ni_{0.5}$	0.34	2.3	0.67
$Co_{0.2}Ni_{0.8}$	0.20	4.0	0.78
80Co:20Pd (mix)	0.34	4.3	0.52
60Co:40Pd (mix)	0.41	3.7	0.53
40Co:60Pd (mix)	0.31	6.3	0.46

agreement with those obtained from the d.c. polarization studies (Table 2).

4. Conclusion

Submicron size powders of Co, Ni and Co–Ni alloy were synthesized by the polyol method using the corresponding metal malonates. Pd powder was obtained by reduction of PdO_x in methanol. The kinetics of the HER in 6 M KOH electrolyte were studied on electrodes made from the pressed powders. The d.c. polarization measurements resulted in a value close to 120 mV for the Tafel slope, suggesting that the HER follows the Volmer–Heyrovsky mechanism. The values of the apparent exchange current density were in the range 1–10 mA cm^{-2}. The a.c. impedance data measured at several over potentials in the HER region resulted in a single semicircle, apparent exchange current density and energy transfer coefficient were evaluated by employing the NLLS fitting procedure. Electrodes made from Co–Pd mixtures were found to be more porous and were more efficient catalysts compared to the individual metal powders and alloys.

Acknowledgement

One of the authors (PE) thanks the Council of Scientific and Industrials Research, Government of India for his research fellowship.

References

1. J. O'M Bockris and S. Srinivasan, *Electrochim. Acta* **9** (1964) 31.
2. S. Trasatti, *in* H. Grischer and C.W. Tobias (Eds), 'Advances in Electrochemical Science and Engineering,' Vol. 2 (VCH, New York, 1992, p. 594.
3. B.E. Conway and G. Jerkiewicz, *J. Electroanal. Chem.* **357** (1993) 47.
4. A. Rami and A. Lasia, *J. Appl. Electrochem.* **22** (1992) 376.
5. J. Divisek, H. Schmitz and J. Balej, *J. Appl. Electrochem.* **19** (1989) 519.
6. I.A. Rat and K.I. Vasu, *J. Appl. Electrochem.* **20** (1990) 32.
7. L. Chen and A. Lasia, *J. Electrochem. Soc.* **139** (1992) 1058.
8. L. Chen and A. Lasia, *J. Electrochem. Soc.* **139** (1992) 3458.
9. P. Los and A. Lasia, *J. Electroanal. Chem.* **333** (1992) 115.
10. J.J. Borodzinski and A. Lasia, *J. Appl. Electrochem.* **24** (1994) 1267.
11. H. Ezaki, T. Nambu, M. Morinaga, M. Udaka and K. Kawasaki, *Int. J. Hydrogen Energy* **21** (1996) 877.
12. K. Lian, D.W. Krirk and S.J. Thorpe, *Electrochim. Acta* **36** (1991) 537.
13. I. Paseka and J. Velika, *Electrochim. Acta* **42** (1997) 237.
14. N.C. Adriana, S.A.S. Machado and L.A. Avaca, *Electrochem. Commun.* **1** (1999) 600.
15. M. Enyo and P.C. Biswas, *J. Electroanal. Chem.* **335** (1992) 309.
16. L.D. Burke and J.K. Casey, *J. Appl. Electrochem.* **23** (1993) 573.
17. N.V. Krstajic, S. Burojevic and Lj.M. Vracar, *Int. J. Hydrogen Energy* **25** (2000) 635.
18. G. Viau, F. Fiévet-Vincent and F. Fiévet, *Solid State Ionics* **84** (1996) 259.
19. H.N. Vasan and C.N.R. Rao, *J. Mater. Chem.* **5** (1995) 1755.
20. J. Prabhuram, R. Manoharan and H.N. Vasan, *J. Appl. Electrochem.* **28** (1998) 935.
21. P. Elumalai, H.N. Vasan, M. Verelst, P. Lecante, V. Carles and P. Tailhades, *Mater. Res. Bull.* **37** (2002) 355.
22. B.A. Boukamp, 'Equivalent circuit users manual' (University of Twent, Enschede, 1989), p. 26.
23. J. Divisek, *J. Electroanal. Chem.* **214** (1986) 615.
24. L. Chen and A. Lasia, *J. Electrochem. Soc.* **138** (1991) 3321.
25. N. Spataru, J-G. Lehelloca and R. Durand, *J. Appl. Electrochem.* **26** (1996) 397.
26. R. Notoya, *Electrochim. Acta* **42** (1997) 899.
27. A.N. Frumkin, *in* P. Delahay and C. Tobias (Eds), 'Advances in Electrochemistry and Electrochemical Engineering', Vol. 3 (John Wiley & Sons, New York, 1963), p. 287.
28. R. Šimpraga, L. Bai and B.E. Conway, *J. Appl. Electrochem.* **25** (1995) 628.
29. R. De Levie, *J. Electroanal. Chem.* **281** (1990) 1.
30. P. Elumalai, H.N. Vasan and N. Munichandraiah, *J. Solid State Electrochem.* **3** (1999) 470.